Multiphysics of seismic analysis and reactive chemical transport analysis for long-term environmental safety evaluation of RC-built hazardous waste landfill

Hiroyuki Ishimori [i)], Kazuto Endo [ii)] , Tomonori Ishigaki [i)],
Kazuo Yamada [iv)] and Masato Yamada [iii)]

i) Senior Researcher, Center for Material Cycles and Waste Management Research, National Institute for Environmental Studies, 16-2, Onogawa, Tsukuba 305-8506, Japan.
ii) Head, Fukushima Branch, National Institute for Environmental Studies, 10-2, Fukasaku, Miharu 963-7700, Japan.
iii) Head, Center for Material Cycles and Waste Management Research, National Institute for Environmental Studies, 16-2, Onogawa, Tsukuba 305-8506, Japan.
iv) Senior Researcher, Fukushima Branch, National Institute for Environmental Studies, 10-2, Fukasaku, Miharu 963-7700, Japan.

ABSTRACT

Multiphysics of seismic analysis and reactive chemical transport analysis were conducted to evaluate the long-term environmental safety of hazardous waste landfills having a reinforced concrete structure. The structure stabilities when huge earthquakes occurred were assessed using seismic analysis. The bending moment generated in the reinforced concreate materials was converted into the crack width, and then the calculated crack width was applied as the boundary conditions of hazardous waste landfill for reactive chemical transport analysis. The results of reactive chemical transport analysis showed the long-term leaching concentration profiles from hazardous waste landfill and specified the factors affecting its environmental safety. This paper finally presents the importance of multi-barrier system consisting of stabilization/solidification techniques and artificial/natural soil sorption layer in order to minimize negative impacts of hazardous waste landfill.

Keywords: RC-built hazardous waste landfill, environmental safety evaluation, multiphysics numerical analysis

1 INTRODUCTION

Hazardous wastes pose a hazard to human health or the environment when improperly managed. They have the extremely high leaching concentrations so that they cannot be disposed directly to regular landfill sites. In Japan, such hazardous wastes are strictly controlled in waste containment facilities having a roof to prevent the wastes from leaching due to rainfall. Japanese hazardous waste containment facilities have been built using waterproof reinforced concrete with thickness of > 350 mm and compressive strength of > 25 MPa. Figure 1 shows one of the hazardous waste containment facilities. The waste containment facilities are divided into several sections which are separated by reinforced concrete, and each section has a capacity with < 250 m^3. Currently, there are 24 facilities in Japan (Tojo et al., 2020).

Material strength of reinforced concrete is gradually deteriorated due to salt damage and carbonation. Salt damage is caused by corrosion of rebars in the concrete, and it is enhanced under the existence of chloride ion. In contrast, carbonation is caused by neutralization of alkali in the concrete exposed to carbon dioxide. As hazardous wastes such as fly ash and sludge have a lot of chloride ion and organic substances for generating carbon dioxide due to biodegradation, respectively, wastes themselves stored in the facilities would lead to deteriorate the reinforced concrete. Its material strength becomes weak.

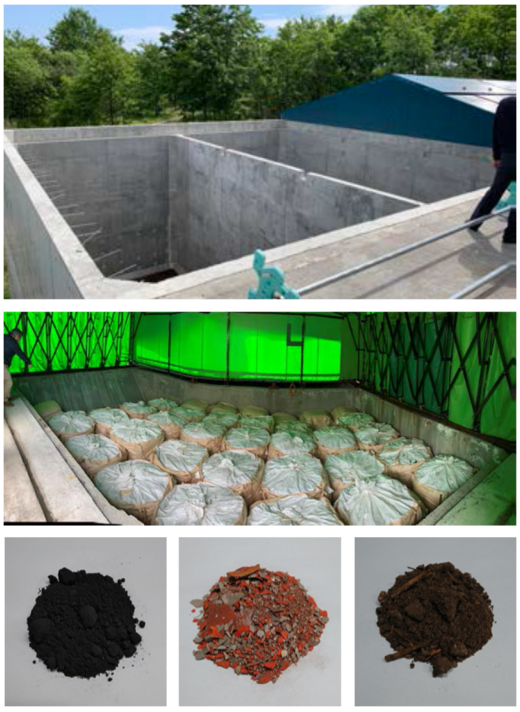

Fig. 1. Example of hazardous waste containment facility in Japan: top figure shows a hazardous waste containment facility under construction, middle figure shows a facility in operation where there is a roof to prevent rainfall permeation and the flexible container bags including the hazardous wastes are disposed, and bottom figure shows the hazardous wastes of fly ash and sludges.

As the results, risks that serious cracks and failures to allow rainfall permeation will be increased.

Huge earthquakes beyond expectation had occurred in Japan. Hence, it is necessary to reassess the structure stability and the containment performance of hazardous waste containment facilities built using reinforced concrete, in consideration of the chemical deterioration due to salt damage and carbonation of reinforced concrete and the external force due to huge earthquake. In this study, multiphysics numerical simulations of seismic analysis and reactive chemical transport analysis were conducted. This paper presents the mathematical models to evaluate the long-term environmental safety for hazardous waste containment facilities and clarifies the importance of multi-barrier system using stabilization/solidification treatment and installation of artificial/natural soil sorption layer to minimize the transport of contaminants leaked from hazardous wastes.

2 THEORY

2.1 Ground deformation analysis

Seismic analysis in this study consisted of the following two steps: (1) ground deformation analysis, and (2) structure analysis as shown in Figure 2. Firstly, the displacements of the ground due to earthquake were calculated using the following wave equation

$$\rho_t \frac{\partial^2 u_z}{\partial t^2} = \frac{\partial}{\partial z}\left(G^* \frac{\partial u_z}{\partial z}\right) \quad (1)$$

where, t is the elapsed time (s), z is the vector in the direction of depth (m), u_z is the displacement (m), ρ_t is the bulk density of soil (kg/m^3), and G^* is the complex stiffness (Pa). The complex stiffness is given as $G^* = G(1+2ih)$, where G is the shear modulus (Pa) and h is the damping factor. The shear modulus, G, and the damping factor, h, have a strain dependency. This study assumed the ground to be sandy loam so that the strain dependencies of G and h were expressed as Figure 3. To calculate the ground displacement, u_z, equation (1) was mathematically solved in frequency domain using SHAKE-91 (University of California, Berkeley). For the initial conditions, all of the ground displacement was set at zero. For the boundary conditions, Fourier spectrums for two earthquakes as shown in Figure 4 were set at the bottom boundary of the domain and the shear stress at the top boundary was set at zero. Level 1 of earthquake motion is defined as being likely to occur during the life-span of the structure. Level 2 of earthquake motion is defined as associated with infrequent rare events that typically involve very strong ground shaking.

2.2 Structure analysis

Secondly, structure stability for a hazardous waste containment facility was evaluated in consideration of the results of previous ground deformation analysis. The structure of reinforced concrete-built hazardous waste containment facility was modeled as one-dimensional

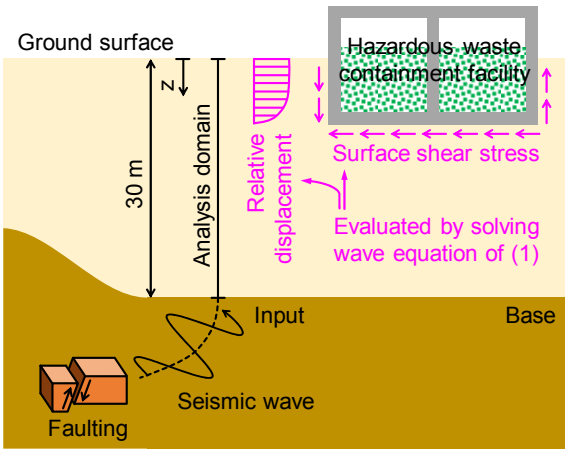

Fig. 2. Overview of seismic analysis.

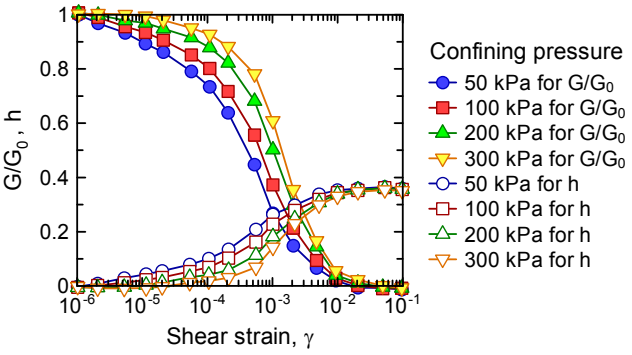

Fig. 3. Nonlinearity of shear modulus and damping factor of soil.

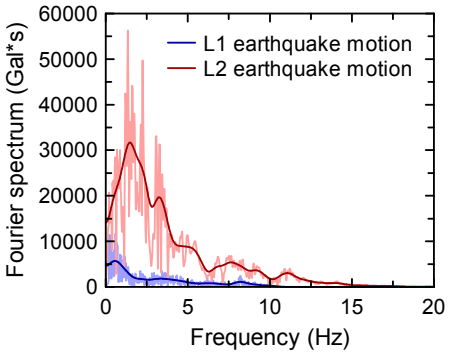

Fig. 4. Characteristics of input seismic waves.

beam elements. The governing equations can be derived from equilibrium of force, and they are expressed as

$$\frac{\partial}{\partial x}\left(EA\frac{\partial u}{\partial x} + N_{ext}\right) = f_x \quad (2)$$

$$\frac{\partial^2}{\partial y^2}\left(EI\frac{\partial^2 v}{\partial y^2} + M_{ext}\right) = f_y \quad (3)$$

where, x is the vector in the longitudinal direction of beam (m), y is the vector in the transverse direction of beam (m), u is the displacement in the longitudinal direction of beam (m), v is the displacement in the transverse displacement of beam (m), E is the Young's modulus (Pa), A is the cross section area of beam (m^2),

I is the second moment of area (m^4), N_{ext} is the external axial force (N), and M_{ext} is the external bending moment (M*m). In addition, f_x and f_y are the body forces (N/m), where they are inertia force or gravity depending on the material density of beam.

Equations of (2) and (3) are used for calculating the displacements, then the axial force, N, and the bending moment, M, are evaluated based on linear elastic theory of $N = EA\,\partial u/\partial x + N_{ext}$ and $M = EI\,\partial^2 v/\partial y^2 + M_{ext}$. Figure 5 shows the boundary conditions. First boundary condition was used to calculate initial axial force and bending moment at state of ordinary by setting N_{ext} and M_{ext} at zero. The calculated axial force and bending moment were set into N_{ext} and M_{ext}, and then second boundary condition was used to calculate the axial force and the bending moment at state of earthquake.

Material strength of reinforced concrete was given as a nonlinear function. Figure 6 is the relationship between the bending moment and the curvature in reinforced concrete, and the slope of the relationship is the stiffness, EI. Points of C, Y, and U in this figure indicate the states of reinforced concrete as shown in Figure 7. The C-point is a state when cracks are generated in the reinforced concrete. The Y-point is a state when the tensile rebars are yielded. The U-point indicates an ultimate state when the concrete breaks due to compression. The relationship between the bending moment and the curvature at each point can be theoretically estimated from equilibrium of force, and the relationship is significantly dependent on the effective cross areas of the concrete and the rebars. Also, the deterioration of reinforced concrete due to salt damage and carbonation can be modelled as the decrease of the effective cross areas of the rebars. It is noted that the carbonation does not directly affect the compressive strength of the concrete. In the carbonation reaction, the calcium hydroxide in the concrete is changed to the calcium carbonate by neutralization of alkali, resulting in denser pore structure and larger compressive strength. However, the carbonation attacks the protective ferric oxide film that forms on the rebars and the corrosion of the rebars start. Therefore, this study only focused on the effects of the carbonation on the corrosion of the rebars, not the compressive strength of the concrete.

2.3 Reactive chemical transport analysis

Reactive chemical transport analysis was conducted to evaluate the chemical concentration distributions in waste containment facility before cracks of reinforced concrete material occurred. This analysis consisted of three parts. First part aimed to evaluate the concentration distributions of carbon dioxide, oxygen, and chloride ion. Second part aimed to evaluate the neutralization depth in the reinforced concrete. Last part aimed to evaluate the corrosion rate of rebars in the reinforced concrete according to electrochemical theory.

The mass balance equations for the carbon dioxide, the oxygen, and the chloride ion in the fully-closed waste containment facility (see Figure 8) were expressed as

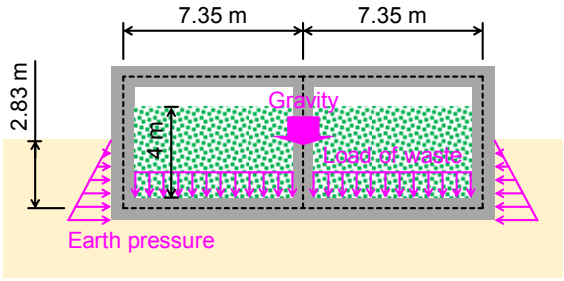

(a) state of ordinary

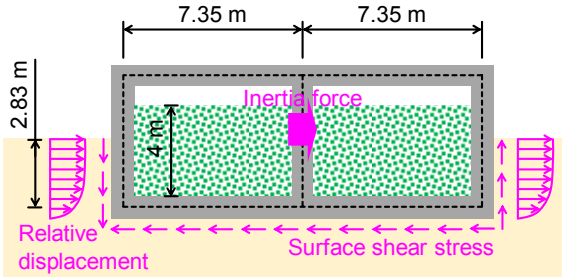

(b) state of earthquake

Fig. 5. Boundary conditions for structure analysis.

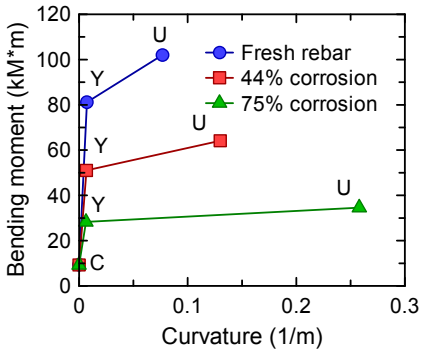

Fig. 6. Material strengths of reinforced concrete with corrosion (thickness = 350 mm).

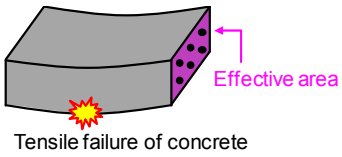

(a) state at point C

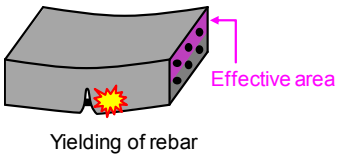

(b) state at point Y

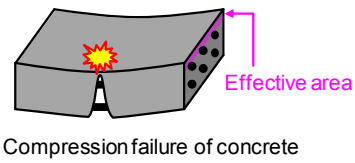

(c) state at point U

Fig. 7. Definition of relationship between moment and curvature.

$$\frac{\partial(c_{CO2}\theta_g)}{\partial t} + \nabla\cdot(-\theta_g\tau D_{mCO2}\nabla c_{CO2}) = R_{CO2} \quad (4)$$

$$\frac{\partial(c_{O2}\theta_g)}{\partial t} + \nabla\cdot(-\theta_g\tau D_{mO2}\nabla c_{CO2}) = R_{O2} \quad (5)$$

$$\frac{\partial(c_{Cl}\theta_w)}{\partial t} + \nabla\cdot(-\theta_w\tau D_m\nabla c_{Cl}) = R_{Cl} \quad (6)$$

where, τ is the tortuosity, c_{CO2} is the carbon dioxide concentration (mol/m^3), c_{O2} is the oxygen concentration (mol/m^3), c_{Cl} is the chloride concentration (mol/m^3), θ_g is the volumetric gas content, θ_w is the volumetric water content, D_m is the molecular diffusion coefficient in water (m^2/s), D_{mCO2} and D_{mO2} are the diffusivity of the carbon dioxide and the oxygen in mixture gas (m^2/s). It is noted that advection effect in equations of (4) to (6) due to pressure gradient was assumed negligible because of the fully-closed analysis domain without cracks.

The source/sink terms were expressed as follows:

$$R_{CO2} = \frac{\rho_d}{M_{CO2}}\left[\frac{\partial W_{doc}^{ar}}{\partial t} + \frac{\partial W_{doc}^{an}}{\partial t}(1-F)\right]\frac{44}{12} \quad (7)$$

$$R_{O2} = -\frac{\rho_d}{M_{O2}}\lambda_{O2max}\frac{W_{doc}}{K_w + W_{doc}}\frac{c_{O2}}{K_{O2} + c_{O2}}W_{doc} \quad (8)$$

where, ρ_d is the dry bulk density of waste (kg/m^3), R_{CO2} is the carbon dioxide generation rate from waste degradation (mol/m^3/s), R_{O2} is the oxygen consumption rate from waste degradation (mol/m^3/s), M_{CO2} and M_{O2} are the molecular weights of carbon dioxide and oxygen (kg/mol), λ_{O2max} is the maximum first order decay rate (1/s), K_w is the half-saturation constant for degradable organic carbon in waste (mg/kg), and K_{O2} is the half-saturation constants for oxygen (mol/m^3). The amount of degradable organic carbon in waste, W_{doc}, related to $\partial W_{doc}/\partial t = -\partial W_{doc}^{ar}/\partial t - \partial W_{doc}^{an}/\partial t$, here W_{doc}^{ar} and W_{doc}^{an} are the aerobic or anaerobic degradation amounts (mg/kg), respectively. They were calculated as

$$\frac{\partial W_{doc}^{ar}}{\partial t} = \frac{c_{O2}}{K_I^* + c_{O2}}k^* W_{doc} \quad (9)$$

$$\frac{\partial W_{doc}^{an}}{\partial t} = \left(1 - \frac{c_{O2}}{K_I + c_{O2}}\right)kW_{doc} \quad (10)$$

where, $k^*$and k are the first-order decay rate in aerobic or anaerobic condition (1/s), respectively. K_I^* and K_I are the half-saturation constant for oxygen in aerobic or anaerobic condition (mol/m^3), respectively. In contrast, the source/sink term for dissolved chloride was defined by the long-term leaching test, and it was formulated as

$$R_{Cl} = \rho_d K t^{-a} \quad (11)$$

where, K and a are the fitting parameters to the result of the serial batch leaching test as shown in Figure 9.

In reinforced concrete, next, the chemical reaction of the neutralization was expressed as $Ca(OH)_2 + CO_2 \rightarrow CaCO_3 + H_2O$. Hence, the formulas are written as

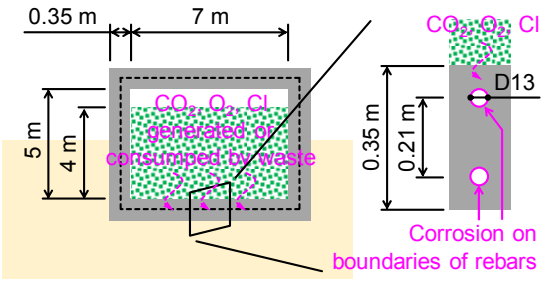

Fig. 8. Analysis domain before cracking or failure.

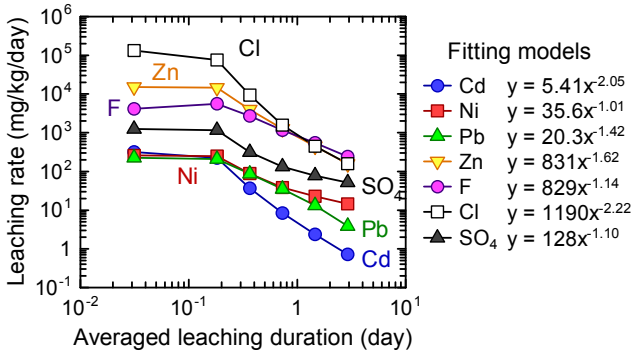

Fig. 9. Example of serial batch leaching test for fly ash

$$\frac{\partial c_{CO2}}{\partial t} = \nabla\cdot(D_{mCO2}\nabla c_{CO2}) - \lambda c_{CO2}c_{Ca(OH)2} \quad (12)$$

$$\frac{\partial c_{Ca(OH)2}}{\partial t} = -\lambda c_{CO2}c_{Ca(OH)2} \quad (13)$$

where, $c_{Ca(OH)2}$ is the concentration of the calcium hydroxide in concrete (mol/m^3) and λ is the second-order reaction rate (m^3/mol/s).

When $c_{Ca(OH)2}$ in the concrete was achieved at zero due to the above reaction, the corrosion of rebars in the concrete started. The corrosion of rebars was modelled as Nernst-Planck equations of

$$\frac{\partial c_i}{\partial t} + \nabla\cdot\left(-D_{mi}\nabla c_i - \frac{z_i D_{mi}}{RT}Fc_i\nabla\phi\right) = 0 \quad (14)$$

$$\nabla\cdot(-\sigma\nabla\phi) = 0 \quad (15)$$

where, i is the index for dissolved oxygen or chloride, c_i is the concentration of species i (mol/m^3), D_{mi} is the molecular diffusion coefficient for species i (m^2/s), z_i is the charge number of species i, R is the gas constant (= 8.31 J/mol/K), T is the absolute temperature (K), F is the Faraday constant (= 96,500 C/mol), ϕ is the electrolyte potential (V), and σ is the electrolyte conductivity (S/m). The corrosion reactions are considered as the boundary conditions on the surface of rebars (see Figure 8). Anode electrode reaction was given as $Fe \rightarrow Fe^{2+} + 2e^-$, and cathode electrode reactions were given as $O_2 + 2H_2O + 4e^- \rightarrow 2OH^-$ and $2H^+ + 2e^- \rightarrow H_2$. Exchange current densities due to their corrosion reactions were expressed according to Tafel's equation of $i_{loc} = i_0 10^{\eta/A}$. Table 1 and Figure 10 show the Tafel parameters (Tong, 2019).

Table 1. Tafel parameters for corrosion reactions of rebar.

Reaction	η (mV)	A (mV)	i_0 (A/m^2)
$Fe \rightarrow Fe^{2+} + 2e^-$	760	410	see Fig.10
$O_2 + 2H_2O + 4e^- \rightarrow 2OH^-$	189	-180	-7.7×10^{-7}
$2H^+ + 2e^- \rightarrow H_2$	1,030	-150	-1.1×10^{-2}

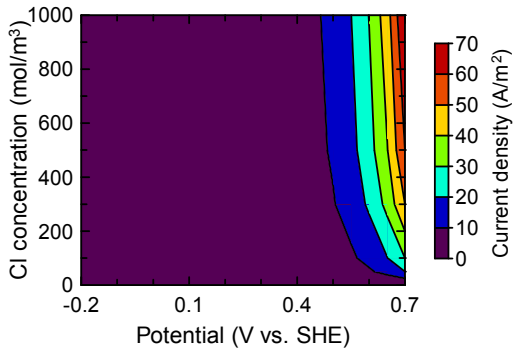

Fig. 10. Polarization characteristics for steel (Tong, 2019)

The boundary values on rebars for equation (15) were given by summation of their current densities. From the results of corrosion analysis consisting of equations (14) and (15), the corrosion rate of rebar can be estimated as

$$m_t = \frac{\Delta m}{\Delta t} = \frac{i_{cor} M}{nF} \tag{16}$$

where, m_t is the corrosion rate of rebar (kg/m^2/s), i_{cor} is the corrosion current density (A/m^2), M is the molecular weight (kg/mol), and n is the stoichiometric coefficient in corrosion reaction. The corrosion rate was used for recalculating the effective area of rebars after corrosion, and the stiffness of the reinforced concrete was modified according to corrosion progress as shown in Figure 6.

2.4 Groundwater flow and transport analysis

After cracking or failure, the waste leachate in the waste containment facility starts flowing out.

Groundwater flow and transport analysis is widely used in geoenvironmental engineering. Detailed theory can be referred from Bear and Verruijt (1987). Water flow and chemical transport in soil environment are solved by the following seepage equation and advection-dispersion equation,

$$\frac{\partial \theta_w}{\partial p_w}\frac{\partial p_w}{\partial t} = \nabla \cdot \left[-\frac{k_{rw} K}{\eta_w} (\nabla p_w + \rho_w g) \nabla z \right] \tag{17}$$

$$(\theta_w + \rho_d K_d)\frac{\partial c_M}{\partial t} = \nabla \cdot (\theta_w D \nabla c_M - u_w c_M) \tag{18}$$

where, p_w is the pore water pressure (Pa), k_{rw} is the relative permeability, K is the intrinsic permeability (m^2), ρ_w is the density of water (kg/m^3), η_w is the viscosity of water (Pa*s), ρ_d is the dry bulk density of soil (kg/m^3), D is the mechanical dispersion coefficient (m^2/s), K_d is the distribution coefficient (m^3/kg), c_M is the heavy metal concentration in water (mol/m^3), u_w is the darcy velocity (m/s), and g is the gravitational acceleration. The k-S-p relation was given by van Genuchten model.

3 CASE STUDIES

Figure 11 shows the overview of numerical studies. Analysis domain consisted of waste containment facility and its surrounding ground. The environment safety for hazardous waste in the facility built using reinforced concrete was evaluated by predicting the concentration of the heavy metal at a monitoring well that was located at the lower reaches of the groundwater. Governing equations described in previous section were solved using Moleman-i plus (Mizuho Information & Research Institute) for seismic analysis and COMSOL MP ver 5.0 (COMSOL, Inc) for reactive chemical transport analysis.

Four numerical studies were performed. Case 1 was when no earthquake occurred for 100 years. Cases 2 and 3 were when L1 or L2 earthquake occurred after 5 years, respectively. Case 4 additionally had a 50-cm sorption layer underlying the waste containment facility. Table 2 shows calculation conditions used in the case studies. Hazardous waste was assumed fly ash shown in Figure 9, and cadmium in the ash was selected as a contaminant.

4 RESULTS

Figure 12 shows the results of numerical simulations. Their graphs indicate the concentration profiles in top or bottom reinforced concrete material in the hazardous waste containment facility. A high-concentration carbon dioxide generated from the waste led both reinforced concrete materials to neutralization within 12 days. Then,

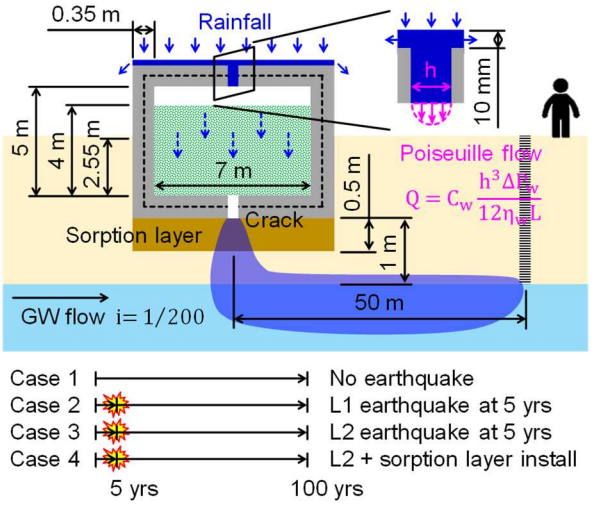

Fig. 11. Analysis domain and analysis conditions for case studies.

Table 2. Main calculation parameters.

Parameter	Value
N-values for ground assuming sandy loam, N	30
Shear wave velocity, V_s	249 m/s
Maximum oxygen consumption rate, λ_{O2max}	4.9×10^{-2} d^{-1}
First-order decay rate in anerobic cnd., k^*	2.0 yr^{-1}
First-order decay rate in anaerobic cnd., k	0.2 yr^{-1}
Second-order reaction rate for carbonation, λ	0.6 m^3/mol/d
Intrinsic permeability for ground, K	1.0×10^{-12} m^2
Distribution coefficient for sorption layer, K_d	300 mL/g

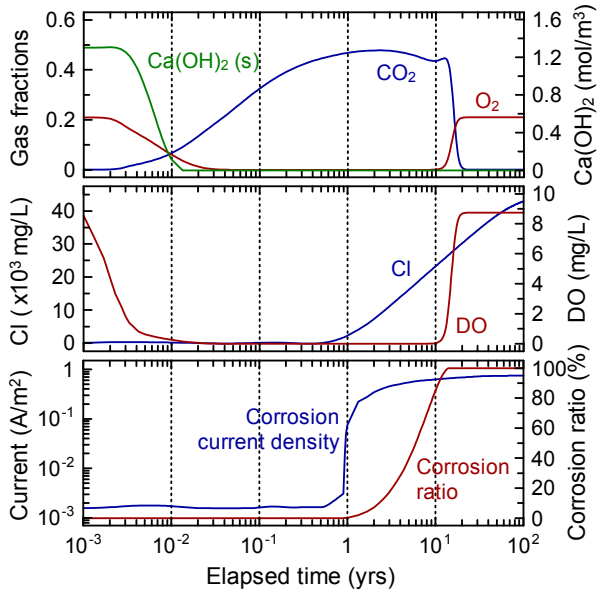

(a) bottom RC material

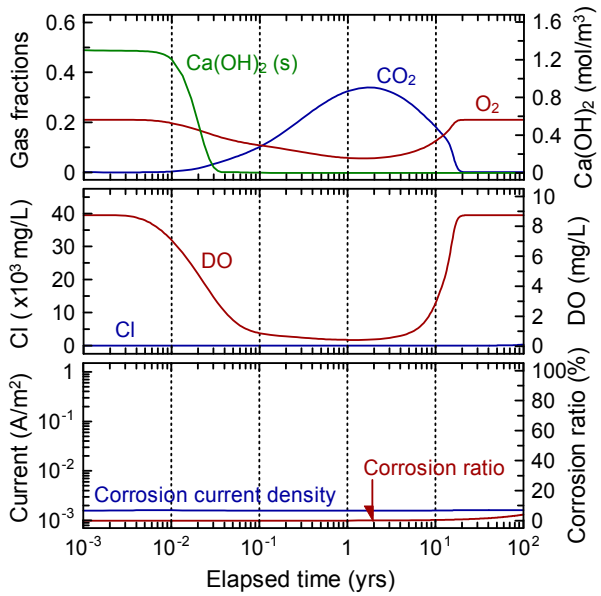

(b) top cover RC material

Fig. 12. Concentration profiles in waste containment facility.

salt damage started. The chloride ion infiltrated only the bottom reinforced concrete. The rebars started to corrode one year later and the corrosion ratio reached 100% after 10 years. In contrast, the corrosion ratio of the rebars in the top cover reinforced concrete was 4% at maximum.

Table 3 shows the results of seismic analysis. In any top cover reinforced concretes, the crack was generated, resulting in the infiltration of rainfall into the hazardous waste containment facility. Whereas, the crack in the bottom reinforced concrete was not generated in Cases 1 and 2 although the deterioration due to carbonation and salt damage were considered. The crack width in Cases 3 and 4 was estimated as 0.11 mm, which was smaller than that in the top cover reinforced concrete.

Figure 13 shows the results of groundwater flow and

Table 3. Results of seismic analysis.

		M_{max} (kN*m)	N (kN)	Failure mode	h^* (mm)	Q^* (mL/d/m)
Case 1	Bottom RC	6.6	39.9	No crack	0	Close bnd.
	Top RC	23.2	11.7	Crack	0.330	2,900
Case 2	Bottom RC	6.2	37.9	No crack	0	Close bnd.
	Top RC	20.9	17.1	Crack	0.291	1,990
Cases 3 & 4	Bottom RC	7.3	25.9	Crack	0.110	Open bnd.
	Top RC	22.2	17.9	Crack	0.306	2,310

* h and Q are estimated from JSCE (2018)

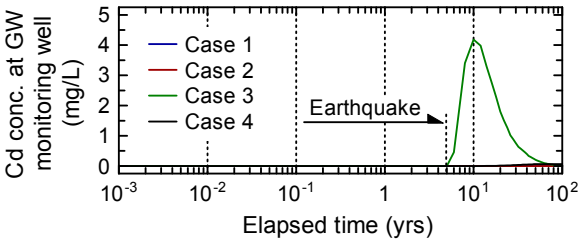

Fig. 13. Cadmium concentration profiles in groundwater

transport analysis for cadmium leached from the waste containment facility. No cadmium appeared in Cases 1 and 2 because the bottom reinforced concrete did not have the crack to leak the cadmium. But, the cadmium was leaked from the crack in Cases 3 and 4 so that the cadmium was transported with groundwater flow and observed in the monitoring well. Sorption layer was effective to prevent the groundwater contamination, and it was an important factor for controlling the long-term environmental safety of hazardous waste landfills.

5 CONCLUSIONS

This paper presented numerical simulation model to evaluate the environmental safety of hazardous waste landfills having a reinforced concrete structure. Multi-barrier system, having the sorption layer additionally installed under RC-built hazardous waste landfill, can retard the transport of contaminants and it was effective to improve their environmental safety.

ACKNOWLEDGEMENTS

This study was supported from the Environment Res. and Tech. Development Fund (JPMEERF20183002) of Environ. Restoration and Conservation Agency of Japan.

REFERENCES

1) Tojo, Y., Ikeda, T., Matsuo, T. and Matsuto T. (2020): The Effect of Inside Circumstance of the Hazardous Waste Landfill on the Leaching Behavior of Harmful Heavy Metals, *International Journal of GEOMATE*, 18(66), 129-134
2) Tong, L. (2019): Numerical Analysis of Corrosion using COMSOL Multiphysics: Modeling of Crevice Corrosion, *COMSOL Conference 2019 Tokyo*, P-19.
3) Bear, J. and Verruijt, A. (1987): Modeling Groundwater Flow and Pollution, *ISBN 978-1-55608-014-2*, Springer.
4) JSCE Concrete Committee (2018): Standard Specifications for Concrete Structures, *ISBN 978-4-8106-0777-2*, JSCE.